Fluorescence Polarization Decay Study of Polymer Dynamics: A Critical Discussion of Models Using Synchrotron Data

Jean Louis Viovy* and Lucien Monnerie

Laboratoire de Physicochimie Structurale et Macromoleculaire (LA CNRS 278), ESPCI, 75231 Paris Cedex 05, France

Jean Claude Brochon

Laboratoire pour l'Utilisation du Rayonnement Electromagnetique, Universite Paris-sud et CNRS, 91401 Orsay Cedex, France. *Received August 5, 1982*

ABSTRACT: The fluorescence polarization decay of polystyrene labeled with anthracene in the middle of the chain is recorded by using cyclosynchrotron radiation as an exciting source. The good performances of this source permit a quantitative comparison of the different expressions for the main-chain orientation autocorrelation functions published in the literature, i.e., the Valeur, Jarry, Geny, and Monnerie (VJGM), Bendler and Yaris (BY), Jones and Stockmayer (JS), Williams and Watts (WW), and Hall and Helfand (HH) models. The different models are discussed on the basis of the goodness of fit, stability on truncation, and physical credibility of the best-fit parameters. At the level of accuracy of these experiments, only the BY, JS, and, to a lesser extent, the HH models seem to account for the orientational dynamics of labeled polystyrene in all the situations investigated. Nevertheless, a generalization of the HH model can be proposed, which makes it more suitable for the fitting of fluorescence experiments but retains the attractive feature of this model, i.e., a clear molecular basis. This modified model reaches the same quality of fitting as the BY and JS models.

I. Introduction

The understanding of polymer dynamics, as an N-body problem, is a difficult task. The first step is the definition of a few statistical quantities, usable on a macroscopic scale and reflecting the main features of the system. Correlation functions are such quantities, and they have been used extensively since the beginning of the century as the necessary intermediary between theory and experiment. Experiments can be classified into two families, depending on the kind of correlation function (CF) they are sensitive to. For instance, light or neutron scattering and diffusion are sensitive primarily to translation correlation functions, while NMR, ESR, the Kerr effect, dielectric relaxation, and fluorescence polarization are sensitive to the orientation CF (OCF). Among this last series, a further distinction can be made, since different experiments are sensitive to different moments of the orientation distribution function (generally, the first or second one). Finally, it is noteworthy that only the transient Kerr effect and fluorescence polarization measure directly the orientation autocorrelation function (OACF) (respectively the first and second moments) in the time domain.

The separation between translational and orientational CF is an oversimplification since the knowledge of one CF generally gives information about the others. Nevertheless, in the case of polymers, the two CF are usually devoted to the investigation of motions on rather different time scales: Due to the flexibility of the polymer chain, the orientation correlation length is smaller than the polymer size, and the OCF reflects mainly the local motions ("wiggling" or conformation changes). Moreover, the time scale of the OCF techniques corresponds rather well to local motions and makes these techniques suitable for their study. On the other hand, the translation CF techniques are generally used to study motions on a larger scale, e.g., overall diffusion, reptation, etc., often classified as "universal behavior". Our knowledge of these behaviors has been greatly improved over the past years, thanks to the concept of reptation and the application of scaling laws. But the understanding of polymer dynamics on a more local scale was less affected by these tools and remains at a rather unsatisfying level.

In particular, several expressions for the OACF derived from different models were proposed during the past years.[1-5] Some of them were applied to experiments with rather equal success.[2-4] For some techniques like NMR or ESR, which need the a priori choice of a model to be interpreted, the problem then arises of what is the most suitable model to use. Until now, no experimental evidence seemed to be able to answer that question. Fluorescence polarization decay, which provides a quasi-continuous sampling of the second-moment OACF on a 3-decade frequency window, is a priviledged tool for a critical discussion of orientational models.

We undertook a series of fluorescence polarization measurements on labeled polystyrene in dilute solutions of various viscosities, using the cyclosynchrotron LURE-ACO at Orsay (France). The different models presently available are reviewed in section II. Following the experimental procedure described in section III, these models are fitted to the data. The results are presented and discussed in section IV. Improvements are proposed and tested in section V.

II. Models for the Orientational Autocorrelation Function of Polymers

It was recognized very long ago that the OCF of a vector fixed to a polymer chain did not obey a simple Perrin law.[6] Phenomenological distributions of correlation times led to OCF that were in better accord with experiments,[1] but the benefit for polymer dynamics was small since they could not be related to a molecular model. The Rouse equation[7] was used first by de Gennes[8] to predict a long-time behavior of the first moment of the OACF

$$M_1(t) \sim t^{-1/2} \tag{1}$$

At the same time, stochastic jump models were developed to take into account the molecular characteristics of a polymer chain. In these models,[9,10] an "elementary motion", involving only a few monomers is chosen and is supposed to occur randomly along the chain. Dubois-Violette et al.[10] showed that de Gennes' result could be recovered on the basis of a chain performing three-bond motions on a tetrahedral lattice. An expression for the

0024-9297/83/2216-1845$01.50/0

second-moment OACF, valid only in the long-time limit, was proposed:

$$M_2(t) = 0.5\langle 3\cos^2\{U_n(0) - U_n(t)\} - 1\rangle \sim \exp(-w_2 t)(\pi w_1 t)^{-1/2} \quad (2)$$

$U_n(t)$ is the orientation of bond n at time t, and w_1 is the elementary jump frequency. The exponential is introduced to take into account out-of-lattice motions. Valeur and co-workers[2] improved this model by the use of static OCF arising from the fixed bond angles. This led to a very general expression for the OACF:

$$M_2(t) = \exp\{(w_1 - w_2)t\}\ \mathrm{erfc}\ \{(w_1 t)^{1/2}\} \quad (3)$$

w_1 is related to the conformational jump frequency and w_2 has the same meaning as in expression 2. erfc is the complementary error function.

Similar correlation functions have been derived by Hunt and Powles[11] within a defect-diffusion model of reorientation in glasses, by Shore and Zwanzig[12] in their treatment of a perpendicular-dipole model for dielectric relaxation, and by Kimmich,[13] who was interested in NMR in polymer melts. The common feature of the four above theories is their master equation, i.e., a one-dimensional defect diffusion equation:

$$dP/dt = W\, d^2P/dx^2 \quad (4)$$

x is a certain distance along the chain, and P is the probability density of defects (here orientation quanta).

The major defect of eq 3 is an unrealistic infinite first derivative at $t = 0$, due to the continuous approximation in the analytical treatment. This was noticed by Jones and Stockmayer,[3] who treated the problem by keeping eq 4 in its discrete form and performing an exact mode analysis on the resulting Hückel matrix arbitrarily truncated. This theory was applied with success to NMR relaxation. The parameter related to the long-time behavior is then the number of three-bond kinetic units taken into account. This number can take integer values only, each one being associated with a different analytical expression for $M_2(t)$. This discrete truncation is arbitrary and may lead to difficulties when applied to real polymers.

An alternate path was proposed by Bendler and Yaris:[4] The introduction of a long-wavelength and a short-wavelength cutoff in the continuous-mode spectrum of eq 4 leads to an expression for $M_2(t)$:

$$M_2(t) = 0.5(\pi/t)^{1/2}(w_1^{1/2} - w_2^{1/2})\{\mathrm{erfc}\ ((w_2 t)^{1/2}) - \mathrm{erfc}\ ((w_1 t)^{1/2})\} \quad (5)$$

where w_1 and w_2 are the arbitrary cutoff frequencies. Expression 5 is easy to compute and has a satisfactory behavior at short times. Nevertheless one remains unsatisfied by this arbitrary cutoff method since it seems difficult to relate the parameters w_1 and w_2 to molecular times.

Recently, Hall and Helfand[5] proposed a model for conformational dynamics taking into account correlated pair transitions and isolated transitions, each occurring at a different rate. By use of Pauli's spin matrix formalism, this model is able to predict conformation correlation functions (CCF) for rather realistic molecular potentials. Unfortunately, such CCF's are no accessible to experiments and can only be obtained in computer simulations. For a simplified case, namely, a chain of two-state elements, Hall and Hefland also derived the OACF for a single bond:

$$M_2(t) = \exp(-w_2 t)\ \exp(-w_1 t) I_0(w_1 t) \quad (6)$$

Table I
Analytical Expressions for the OACF Used throughout the Paper

ref	abrev	expression
1	WW	$r(t) = r_0\ \exp\{(-t/\tau_1)^\beta\}$
2	VJGM	$r(t) = r_0\ \exp\{(1/\tau_1 - 1/\tau_2)t\} \times \mathrm{erfc}\{(t/\tau_1)^{1/2}\}$
3	JS[a]	$r(t) = r_0 \sum_{i=1}^{n} a_i \exp(-t/\tau_i)$
4	BY	$r(t) = 0.5 r_0 (\pi/t)^{1/2}(\tau_2^{-1/2} - \tau_1^{-1/2}) \times \{\mathrm{erfc}((t/\tau_1)^{1/2}) - \mathrm{erfc}((t/\tau_2)^{1/2})\}$
5	HH	$r(t) = r_0\ \exp(-t/\tau_2) \times \exp(-t/\tau_1) I_0(t/\tau_1)$
6	IR	$r(t) = r_0\ \exp(-t/\tau_1)$
23	RR	$r(t) = r_0\{(1-\beta)\exp(-t/\tau_1) + \beta\}$
25	WH	$r(t) = r_0\{(1-a) \times \exp(-t/\tau_2 - t/\tau_1) I_0(t/\tau_1) + a\}$
	GDL	$r(t) = r_0\ \exp(-t/\tau_2 - t/\tau_1) \times \{I_0(t/\tau_1) + I_1(t/\tau_1)\}$

[a] The values for τ_i and a_i are tabulated in ref 3.

I_0 is a modified Bessel function of order 0 and w_1 and w_2 are associated, respectively, with correlated and isolated jumps. Expression 6 has the correct short-time limiting behavior.

All the correlation functions fitted in the present paper are summarized in Table I. The last four expressions will be introduced later.

III. Experimental Section

Principle. A fluorescence probe is covalently coupled in the middle of a polymer chain, with its transition moments tangent to the skeleton. This probe is excited by a nanosecond pulse of vertically polarized light, and the emitted light is recorded as a function of time in both parallel and perpendicular polarization. Under suitable conditions of wavelength, the emission anisotropy

$$r(t) = \{I_v(t) - I_h(t)\}/\{I_v(t) + 2I_h(t)\} \quad (7)$$

is proportional to the second-moment OACF of the transition moment:

$$r(t) = r_0 M_2(t)/M_2(0) \quad (8)$$

where the fundamental anisotropy r_0 is a molecular parameter related to delocalization, which must be fitted together with $M_2(t)$. Thus fluorescence polarization decay experiments allow a measurement of the OACF directly in the time domain in a quasi-continuous manner. This makes this technique particularly suitable for precise comparison of nonexponential anisotropy decays.

The main limitations of the technique are due to the following: (i) a finite frequency window imposed by the fluorescence lifetime of the label (for high-precision measurements, the reorientation times must have the same order of magnitude as the fluorescence lifetime); (ii) a perturbation of polymer motions by the probe (it has been demonstrated previously[15] that for small labels (like anthracene) and solvents with usual viscosities the motion of the label reflects mainly the properties of the chain); and (iii) an experimental precision limited by the finite width and the instabilities of the pulses and statistical errors. The use of synchrotron radiation as excitation source greatly reduces these disadvantages and leads to a precision out of reach of conventional sources.

Apparatus. The experiments were performed on the A3 beam line of the cyclosynchrotron LURE-ACO. The apparatus has been described elsewhere[5] and we shall only recall the characteristics of the source.

The saphire window on the port allows a continuous wavelength spectrum from 1400 to 8000 Å: Thus the excitation wavelength can be freely selected to match absorption peaks of the label and

Table II
Viscosities of the Ethyl Acetate–Tripropionin Mixtures Used as Solvent

% tripropionin	sample no.	viscosity, cP
0.0	1	0.43
79.8	2	2.28
94.0	3	5.40

to avoid absorption by unwanted fluorescent species (impurities, polymer chain, and solvent). Since the pulse shape of the synchrotron emission is invariant with wavelength, the excitation pulse can be recorded by using scattered light at the selected emission wavelength to avoid deconvolution errors arising from the so-called "color effect" of the photomultiplier.

The high flux allows a precise monochromation in both excitation and emission and short sampling times. The variation of the characteristics of the electronics during the sampling are then minimized.

A quasi-Gaussian and narrow pulse is used (the full width at half-maximum is typically 1 ns). Due to the principle of the synchrotron (control of the pack shape by a high-frequency cavity), the jitter in the position and shape of the exciting pulse is very low and negligible with respect to the fluctuations in the transient time of the photomultiplier. The intensity of the source decays exponentially with a lifetime superior to 10 h. It can be measured independently to correct the data.

A short period is used (73 ns in one-bunch mode). The last property ensures single photoelectron counting but it can be a disadvantage for long decays. We checked that in the present series of experiments the resulting decay overlap is negligible.

The excitation wavelength is selected by a double holographic grating monochromator, the emission wavelength by a single holographic grating, and polarizations by glazebrook prisms. The transmission of the emission monochromator in both polarizations was calibrated by recording I_v and I_h for anthracene in low-viscosity solvents (toluene and ethyl acetate). The correction factor is obtained with a 0.005 precision by

$$c = \int_{t_1}^{t_2} I_v^{\text{measd}} / I_h^{\text{measd}}\, dt \tag{9}$$

with t_1 large enough to ensure complete depolarization by Brownian rotation.

Samples. In order to achieve good precision and unambiguous interpretation, we chose a well-studied system: Polystyrene labeled with anthracene in the middle of the chain.[15,16] The sample was prepared by Valeur.[16] Its molecular weight is 57 000. We used 0.1 OD solutions in different mixtures of ethyl acetate and tripropionin (glyceryl tripropionate). The temperature for all experiments was 25 + 0.2 °C. The excitation and emission wavelengths were set respectively to 385 and 448 nm, and the resolution was 4 nm.

Data Reduction. In order to turn the high quality of our instrument to the best account, a particularly careful data treatment was necessary. It was performed on the CNRS-CIRCE IBM360/170-Amdahl V7 computer system. We used a deconvolution procedure[17] based on nonlinear least-squares analysis, including some recent improvements of fluorescence data treatment or features specific to our experiments.

Let $I_v(i)$ and $I_h(i)$ represent the raw experimental histograms for vertically and horizontally polarized emitted light. i, an integer variable, is the channel number and can be related to elapsed time by

$$t = (i - 1)\tau; \qquad 1 < i < N \tag{10}$$

where τ is the channel width.

Due to the high repetition rate of synchrotron pulses, the ratio of the number of fluorescence photons to the number of pluses is low, and a background due to the dark current of the photomultiplier must be subtracted from the experimental histograms, leading to

$$I'_v(i) = I_v(i) - B_v$$
$$I'_h(i) = I_h(i) - B_h \tag{11}$$

Since the pulse $P(i)$ is not a δ function, the emission anisotropy is not related to the I's directly via eq 2 but via the convolution products:

$$I'_v(i) + 2cI'_h(i) \# S(I) = s(i)*P(i) \tag{12}$$
$$I'_v(i) - cI'_h(i) \# \{r(i)s(i)\}*P(i) \tag{13}$$

where $s(i)$ is the true decay of the fluorescence intensity, and the symbol # implies best-fit comparison. As is apparent in eq 13, the fitting of $r(i)$ requires previous knowledge of $s(i)$, which can also be fitted via eq 12. Unfortunately, in the case of labeled polymers, the decay of fluorescence intensity is definitely nonexponential This is attributed to slow local fluctuations in the chemical environment of the probe, but no theoretical expression for $s(i)$ is available at the present time. We thus use for $s(i)$ an arbitrary sum of three exponentials. This number of exponentials has no physical meaning. But it has been proved[18] to be a good curve-fitting expression for decays not too far from an exponential. A higher number of parameters generally does not reduce significantly χ^2 but endangers convergence in the case of real data.

In order to compare different models for $r(t)$ and discuss more easily their possible deviation from experimental data, it is convenient to use instead of eq 13

$$\{I'_v(i) - cI'_h(i)\}/\{I'_v(i) + 2cI'_h(i)\} = R(i) \# \ldots \# \{(r(i)s(i))*P(i)\}/S(i) \tag{14}$$

The "experimental anisotropy" $R(i)$ tends to $r(i)$ when the excitation pulse tends toward a δ function. Expressions for the standard deviations of $S(i)$ and $R(i)$ have been given by Wahl[17] and can be easily modified to take into account the subtracted background, since

$$\text{var}\,\{I'_{v,h}(i)\} = I_{v,h}(i) \tag{15}$$

The iterative least-squares optimization is performed by the ZXMIN subroutine of the IMSL library.[19] This subroutine is based on a quasi-Newton algorithm[20] and needs no analytical expression for the derivative of the fitted functions. In order to optimize the steps in the exploration of the χ^2-hypersurface and the precision on the final parameters, $r(t)$ and $s(t)$ are fitted in an arbitrary system of units scaled to reasonable initial values of the parameters.

The variance–covariance matrix is computed in order to check the reliability and precision of best-fit parameters.[21] Finally, three further improvements were applied: subtraction of a "blank" histogram, obtained form a solution of unlabeled polymer, calculation of the decay overlap (the effect of these two corrections was negligible for this series of experiments), and quantization correction. In single-photon-counting experiments, the sampling function is not a Dirac comb, but a comb of double-step functions of width τ. This introduces in the histograms a deformation, especially in the "rise" part of the excitation and fluorescence histograms. Following the ideas recently presented by Bouchy et al.,[22] we developed a corrected convolution algorithm that gives access to the information contained in the first points of the experimental decay. The subsequent increase in the effective frequency window provided essential arguments for a refined discussion of models.

IV. Results

The different expressions for the OACF used in the present paper are gathered in Table I. Our concern is, of course, the discussion of polymer models, and exponentials are not relevant a priori. But to decide if a model is physically significant, one must ensure that any other arbitrary model with the same number of parameters will not fit the data as well. Thus we shall also compare our data to the isotropic rotation (IR)[6] and restricted rotation (RR)[23] models, which lead respectively to monoexponential and exponential-plus-background OACF's (see Table I). For the sake of terseness, results for the complete set of models will be presented only for sample 3 (Tables III and IV). The same features are present for the other samples, and only results directly useful for the discussion are summarized in Tables V and VI. Unless theoretical work

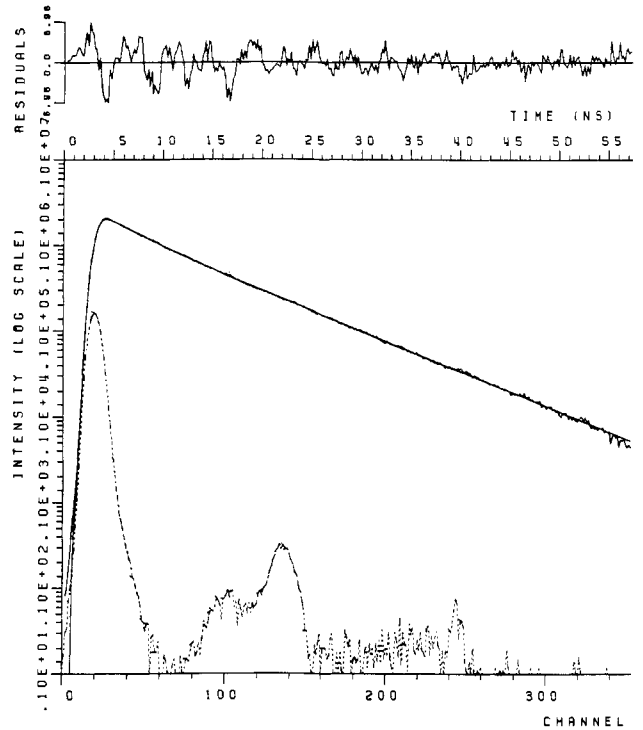

Figure 1. Reconvoluted best-fit three-exponential decay (sample 3) (channel width: 0.162 ns).

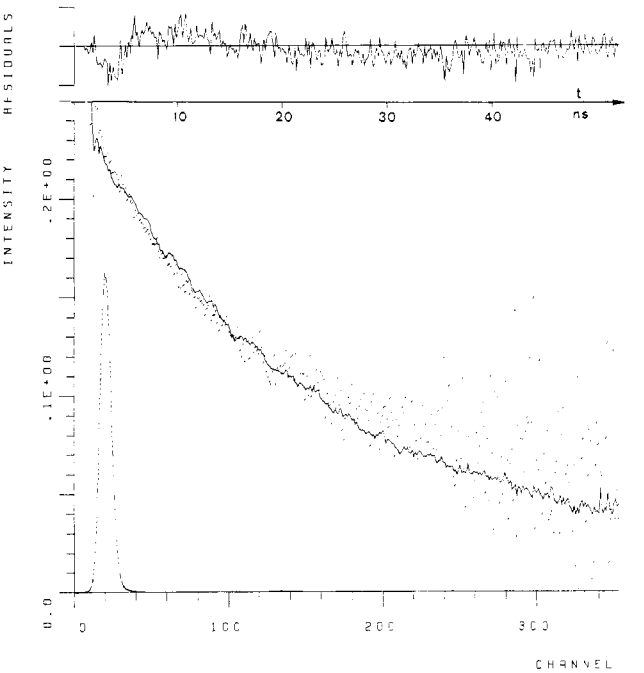

Figure 2. Reconvoluted best-fit anisotropy using the IR model (channel width: 0.162 ns).

most often uses characteristic frequencies, we found that experiments performed in the time domain are more clearly understood in terms of characteristic times. Thus, numerical results are presented in terms of such characteristic times $\tau_i = 1/w_i$.

The total intensity $s(t)$ is not our main concern, but we present it in Figure 1 together with the best-fit and the weighted residuals to show that the arbitrary three-exponential approximation described in the previous section is reasonable: Observation of the residuals reveals no systematic deviation.

The experimental anisotropy $R(t)$ for models IR, RR, and WW is presented in Figures 2–4, respectively. The

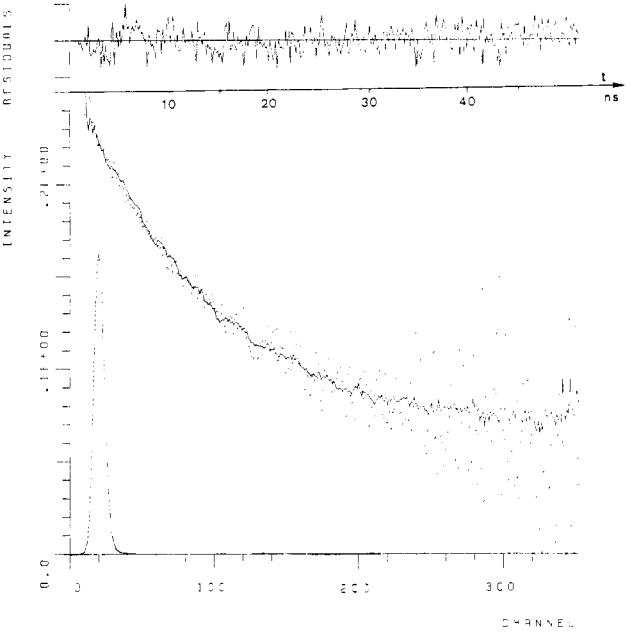

Figure 3. Reconvoluted best-fit anisotropy using the VJGM model (channel width: 0.162 ns).

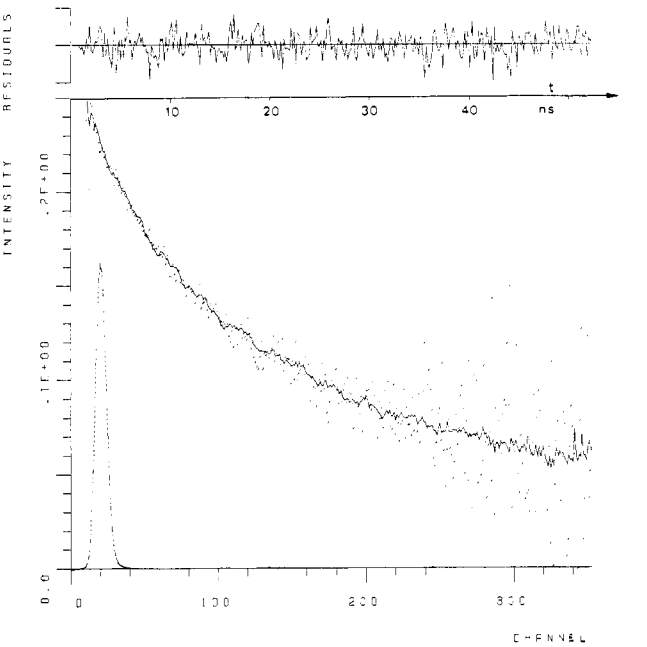

Figure 4. Reconvoluted best-fit anisotropy using the WW model (channel width: 0.162 ns).

inadequacy of the IR model is evident, and some systematic deviations are still apparent for the RR model (compare Figure 3 to Figure 4). But the polymer models lead in any case to rather equivalent weighted residuals, and we did not feel it was necessary to represent them. Thus comparison of the models must be based on more quantitative tools. The reduced sum of residuals χ^2 is the first of these tools. On that account, significant discrepancies can be observed (Table III).

It has to be pointed out that the values of χ^2 appearing in the "experimental anisotropy" deconvolution procedure also take into account the statistical deviations in the previously fitted decay. The anisotroy only contributes to a small part of the computed χ^2. But since the same fitted decay is used with the various models for anisotropy, very small variations of χ^2 can be considered as significant, provided that they are reproducible. On that account, the

Table III
Best-Fit Parameters for Sample 3[a]

model	r_0	τ_1, ns	τ_2, ns	τ_2/τ_1 (or β)	χ^2
IR	0.219	26.8			1.833
RR	0.224	16.5		$\beta = 0.246$	1.129
WW	0.233	28.2		$\beta = 0.764$	0.978
VJGM	0.238	179	43.7	0.24	1.045
JS, 5 bonds	0.228	34.9			0.995
JS, 9 bonds	0.229	34.1			1.044
JS, 13 bonds	0.230	33.8			1.047
BY	0.225	7.54	558	74	1.000
HH	0.225	20.5	10^6	6×10^4	1.017

[a] Fitting window: 0.5/48 ns.

results emphasize clearly the inadequacy of exponential models and the very specific character of polymer dynamics.

For the full-range fit, the VJGM model always leads to higher χ^2's than others. This is not surprising since the slope at time zero of expression 3 is not physically reasonable. Nevertheless, to our knowledge, it is the first time that this theoretical weakness is demonstrated by experimental results.

Interesting information may also be derived from the values of the fitted parameters. At the precision of fitting, all models excpet the WW and VJGM models in some cases lead to values for r_0 similar to and consistent with previous data.[16,24] The deviations for the WW model will be discussed later.

τ_1 and τ_2 obtained in the VJGM model are very surprising: For full-range fitting (Table III), τ_1 is greater than τ_2, which is not consistent with the idea at the basis of the model, i.e., the hypothesis that τ_2 is related to motions spread over a distance greater than the conformational sequence related to τ_1. This anomaly can be explained by the infinite slope at time zero: Even with a high value of τ_1, the VJGM OACF decays too rapidly at short times. It is visible in Figure 5, where the best-fit VJGM OACF

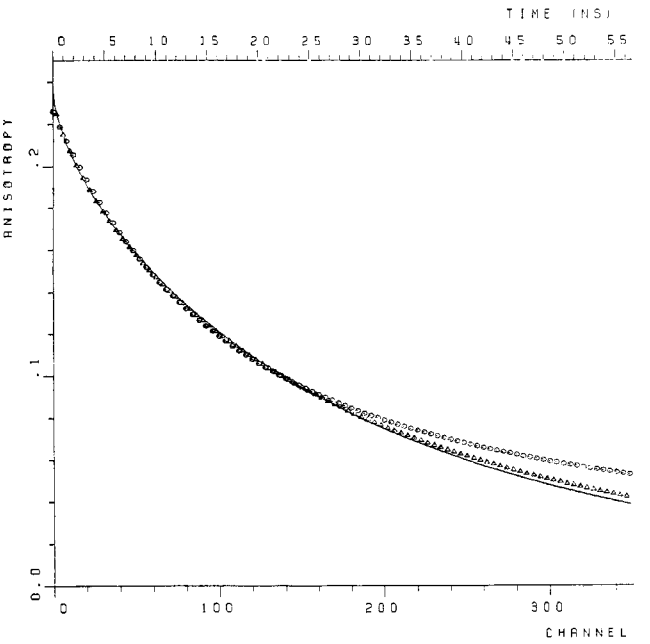

Figure 5. Comparison of the best-fit anisotropies obtained following the VJGM (continuous line), BY (circles), and WW (triangles) models (channel width: 0.162 ns).

(continuous line) is presented together with the BY (circles) and WS (triangles) OACF's: The VJGM line has the steepest slope at the origin.

Decreasing τ_1 would increase this effect and increase χ^2. This cannot be "accepted" by the least-squares program. Then, τ_2 must account for the two processes (conformational jumps and long-range fluctuations), and its best-fit value is greater than that obtained with the BY model. The results in Table IV demonstrate clearly that the unphysical values of τ_1 and τ_2 in Table III are a consequence of the anomalous short-time behavior of the erfc function. When only the end of the decay is retained, τ_1 and τ_2 tend

Table IV
Best-Fit Parameters for Sample 3 for Various Short-Time Truncations

model	window, ns	r_0	τ_1, ns	τ_2, ns	τ_2/τ_1 (or β)	χ^2
RR	0.5/48	0.224	16.45		$\beta = 0.246$	1.129
	8.9/48	0.211	19.3		$\beta = 0.194$	0.999
	14.7/48	0.205	21.4		$\beta = 0.170$	0.999
WW	0.5/48	0.233	28.25		$\beta = 0.764$	0.978
	4/48	0.234	28.1		$\beta = 0.750$	1.000
	8.9/48	0.268	23.1		$\beta = 0.607$	
VJGM	0.5/48	0.238	179	43.7	0.24	1.045
	8.9/48	0.273	36.3	62.0	1.71	0.980
	14.7/48	0.356	12.2	81.4	6.67	0.983
JS, 5 bonds	0.5/48	0.228	34.9			0.995
	8.9/48	0.232	33.74			0.957
BY	0.5/48	0.225	7.54	558	74	1.000
	8.9/48	0.227	7.68	476	62	0.957
HH	0.5/48	0.225	20.5	10^6	6×10^4	1.017
	4/48	0.224	21.2	1391	66	1.050
	8.9/48	0.225	21.2	1359	64	0.960

Table V
Best-Fit Parameters for Sample 3 for Various Long-Time Truncations

model	window, ns	r_0	τ_1, ns	τ_2, ns	τ_2/τ_1 (or β)	χ^2
BY	0.5/25	0.227	6.67	3000	450	1.080
	0.5/48	0.225	7.54	558	74	1.000
	0.5/57	0.226	7.68	480	63	1.046
HH	0.5/25	0.225	20.6	11.6×10^4	747	1.147
	0.5/48	0.225	20.5	10^6	6×10^4	1.017
	0.5/57	0.225	21.4	717	33.5	1.065
JS, 5 bonds	0.5/25	0.228	35.1			1.098
	0.5/48	0.228	34.9			0.995
	0.5/57	0.228	34.7			1.039

Table VI
Best-Fit Parameters for Sample 1

model	window, ns	r_0	τ_1, ns	τ_2, ns	τ_2/τ_1 (or β)	χ^2
RR	4/24	0.166	2.76		$\beta = 0.018$	1.337
WW	0.5/24	0.725	1.81		$\beta = 0.712$	0.972
	4/24	0.210	2.05		$\beta = 0.740$	1.018
VJGM	4/24	0.171	147	3.26	$\beta = 0.002$	1.436
JS, 5 bonds	0.5/24	0.247	1.99			0.995
BY	0.5/24	0.200	0.857	8.40	9.8	1.057
	4/24	0.181	1.149	7.17	6.2	1.050
HH	0.5/24	0.199	2.55	6.71	2.62	1.062
	4/24	0.187	3.56	5.99	1.68	1.049

Table VII
Best-Fit Parameters for Sample 2

model	window, ns	r_0	τ_1, ns	τ_2, ns	τ_2/τ_1 (or β)	χ^2
RR	4/57	0.210	10.8		$\beta = 0.176$	1.210
WW	0.5/57	0.231	14.5		$\beta = 0.691$	1.088
VJGM	4/57	0.226	85	25	0.29	1.247
JS, 5 bonds	4/57	0.222	17.67			1.111
BY	0.5/57	0.217	4.28	172	40	1.113
	4/57	0.220	4.47	134	30	1.135
HH	0.5/57	0.216	12.3	144	11.7	1.135
	4/57	0.214	13.6	100	7.3	1.137

to reasonable values. But then, r_0 becomes too large. Thus these experiments demonstrate clearly that the VJGM model is a good long-time approximation but cannot be applied to describe the first steps of the relaxation. As a matter of fact, this explains also well why this model has been used without trouble in previous experiments:[15,16] Lower precision at short times automatically performed the short-time truncation!

The stability of parameters to variation of the experimental window is indeed a severe trial for a theory, and it can be used also to discuss other models. In particular, it is noteworthy that the WW empirical expression, which sometimes leads to unrealistic values for r_0, also leads to larger variations of the parameters on truncation (see Tables IV, VI, and VII).

For sample 3, changing the short-time fitting truncation by 9 ns induces a 0.035 variation in r_0 (for comparison, the corrsponding variation for the HH or BY model is 0.001). The variation of β from 0.764 to 0.607 is also unacceptable, since this parameter is logarithmic. The results for the lowest viscosity solution (sample 1, Table VI) is even worse, since r_0 varies from 0.21 to 0.72 when the truncation is varied by 4 ns (the corresponding variation for the HH or BY model is about 0.02). Thus, in spite of its very good fitting ability (in most of the cases it leads to the best values for χ^2), this model is not the most suitable one to study polymers since the associated parameters may vary a lot, depending on the experiment and its frequency window. Moreover, they are difficult to relate to molecular quantities.

As pointed out previously, the JS model is not very convenient to use in curve fitting, since each value of the number-of-bonds parameter leads to different expression for the OACF. Nevertheless, we fitted separately the JS expressions for 1, 5, 9, and 13 bonds (further increase in the number of bonds does not modify significantly the OACF, as can be checked in Figure 6. It is noteworthy that the "1-bond" case corresponds to a single exponential.

The best values of χ^2 are very satisfying (respectively 1.05, 1.11, and 0.99 for samples 1, 2, and 3) and are obtained for the "5-bonds" expression. This very low value probably indicates that the "bond" in the JS model does not correspond to a real chemical bond in the chain but to a certain "unit" including several bonds. The exact

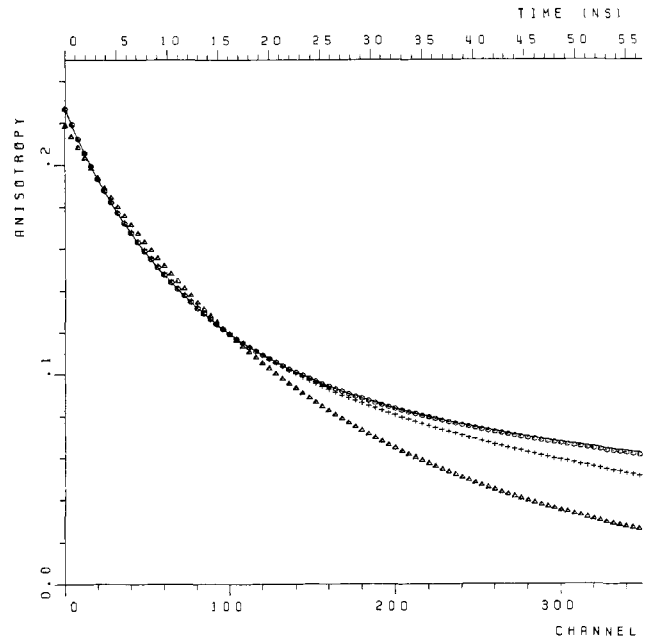

Figure 6. Comparison of the best-fit anisotropies obtained following the JS model for 1 (triangles), 5 (crosses), 9 (circles), and 13 (continuous line) bonds (channel width: 0.162 ns).

nature and size of this unit seem difficult to determine presently. In spite of that and the difficulties raised by the discrete nature of the model, the good values of and the stability of the parameters on short-time and long-time truncation (see Tables IV and V) indicate that the model accounts correctly for the dynamics of polystyrene. For all the truncations tried, the best-fit number of equivalent units remained 5.

The values of χ^2 and the stability on short-time truncation of the parameters obtained with the BY model are also satisfying and make this model suitable for deconvolution of data. Nevertheless, it is worth noticing that truncation of the long-time part of the decay increases τ_2 up to nonsignificant values (see Table V). This probably happens because most of the information about τ_2 is contained in the long-time part of the decay. But these observations are difficult to interpret on a molecular basis: the theoretical problem pointed out in the Introduction remains and the best-fit cutoff frequencies seem difficult to interpret quantitatively in terms of molecular motions.

The HH model, which relies on a clearer molecular basis, also leads to instability upon long-time truncation. For the highest viscosity sample (Table V), only the maximum fitting window leads to a significant value for τ_2. This indicates that the diffusive term accounts almost entirely for the first 50 ns of the decay. Indeed, fixing w_2 to zero increases χ^2 from 1.065 to 1.067, which is negligible. Following the molecular model underlying the HH expression, this would indicate that the isolated jumps are very rare relative to the correlated diffusive ones.

But one must also notice that the HH model does not fit to our experiments as well as the BY or JS models. The higher values of χ^2 observed systematically for all fitting windows and samples may have a physical meaning. It is thus worth recalling that the HH model is derived on a very local molecular basis, i.e., conformational jumps on a chain without pendant groups. Our experiments are performed on labeled polystyrene, and the pendant phenyl groups as well as the anthracene label may perturb slightly the motion of the chain so that more phenomenological models fit the data better.

V. Further Discussion: Generalized Diffusion and Loss Model

To overcome these difficulties we are interested in an expression for the OACF that retains the attractive molecular basis of the HH model but takes into account the somewhat more global character of fluorescent probing. To fit computer simulations, Weber and Helfand (WH) recently supplemented the HH expression by an exponential term,[25] which leads to

$$r(t) = r_0\{(1 - a)\exp(-w_1t - w_2t)I_0(w_1t) + a\exp(-w_3t)\} \quad (16)$$

At the present state of experimental precision, such an expression has too many free parameters to be fitted significantly to the anisotropy decay. But in the frequency window explored here, w_3, which is supposed to be lower than w_2,[25] can be approximated by zero, thus leading to a four-parameter OACF (WH, Table I). When fitted to the data, even this simplified expression could not lead to unambiguous and independent values for w_2 and a, indicating that, at the present state of experimental and computational precision, the bottom of the well in that case is too flat to define precisely enough the two parameters. Moreover, fitting was improved only very slightly by this fourth parameter. For instance, in sample 3, χ^2 was lowered from 1.017 to 1.011 when passing from the HH to the WH model, while the BY value is 1.000. Thus Weber and Helfand's generalization is not able to account better for our observations than the previous HH model.

If, as we suggested at the end of section IV, the relatively bad fit of the HH model is due to pendant groups and label, improvements must be searched for mainly in the short-time part of the OACF, and the inefficiency of the WH term is not surprising. Alternately, we suggest that the OACF for real and labeled polymers may be represented by the generalized diffusion and loss expression

$$r(t) = \tau_0\exp(-w_1t - w_2t)I_0(w_1t) + \sum_{i=1}^{n} a_iI_i(w_1t) \quad (17)$$

where I_i is a modified Bessel function of order i, and a_i is a rapidly decreasing function of t. Theoretically, this is supported by the expression given by Hall and Helfand[5] for the orientational cross-correlation function for two bonds separated by j bonds:

$$c(j,t) = \exp(-w_2t - w_1t)I_{|j|}(w_1t) \quad (18)$$

Equation 17 can then express the fact that pendant groups or labels mix somewhat the motions of neighboring bonds. From a practical point of view this addition of higher order Bessel functions smoothens the OACF, which is also consistent with the idea that short-time diffusive behavior is partially hidden by heavy pendant groups.

For reasons similar to these discussed about the WH expression, stable and quantitative fitting of extra parameters a_i is not possible due to experimental precision. But numerous trials indicated that a major improvement was obtained with a single first-order Bessel function and that the order of magnitude of a_1 for the best fit was 1. Thus we fitted all data with the simplified generalized diffusion and loss (GDL) expression:

$$r(t) = r_0\exp(-w_1t - w_2t)\{I_0(w_1t) + I_1(w_1t)\} \quad (19)$$

Table VIII
Best-Fit Parameters for the GDL Model for All Samples

sample	window, ns	r_0	τ_1, ns	τ_2, ns	τ_2/τ_1 (or β)	χ^2
3	0.5/25	0.227	10.40	188	11.1	1.069
	0.5/48	0.226	12.20	135	11.1	0.986
	0.5/57	0.226	11.46	127	11.1	1.029
	4/48	0.226	12.46	132	10.6	1.021
	9/48	0.229	12.06	128	12.0	0.954
1	0.5/24	0.205	1.31	5.61	4.28	0.983
	4/24	0.192	1.80	5.34	2.98	1.018
2	0.5/57	0.218	6.70	62	9.3	1.114
	9/57	0.230	6.07	58	9.6	1.135

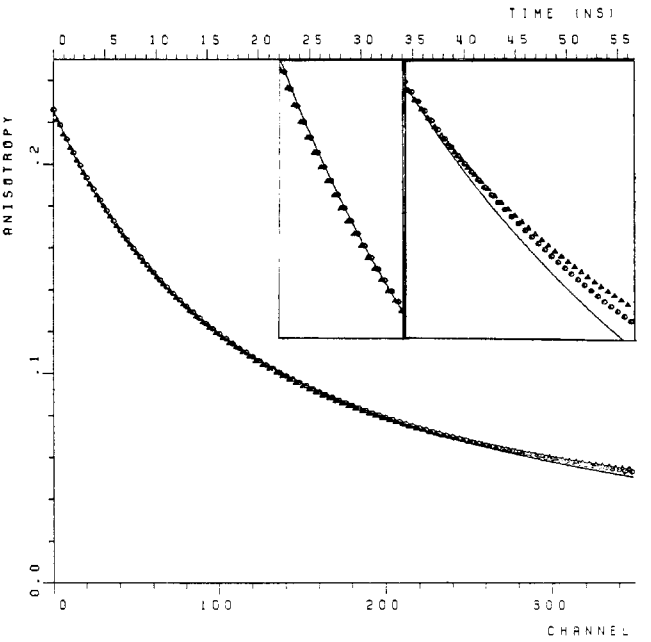

Figure 7. Comparison of the best-fit anisotropies obtained following the BY (circles), HH (triangles), and GDL (continuous line) models (channel width: 0.162 ns). For easier visualization, the inserts represent portions of the plots with a five-times expanded verticle scale (the vertical shift is arbitrary).

The numerical results are collected in Table VIII and the following features can be noticed: χ^2 is significantly improved relative to the HH model and reaches values generally better than the BY and JS models (compare to the results in Tables III–VII); the three parameters r_0, τ_1, and τ_2 are physically reasonable and stable on any kind of truncation; for the three samples, the best-fit value of r_0 is close to the HH one, and τ_1 is about half the HH value.

In Figure 7, the best-fit OACF for sample 3 using the GDL model (continuous line) is compared to the best fit for the HH (triangles) and BY (circles) models. The three curves are indistinguishable at short times. This is merely a consequence of the high weighting of this part of the decay due to an increase of noise at long time. This weighting strongly enforces good fitting at short times, and slight inadequacies of models will be emphasized in the 10–60-ns range. The GDL line remains rather close to the HH one, but its somewhat smoother shape leads to visible deviations beyond 15 ns, which are responsible for the improvement in χ^2.

VI. Conclusions

The diffusive nature of the orientation relaxation in flexible polymers introduces in the orientation autocorrelation function features that can be accounted for only by specific models. Synchrotron-excited fluorescence polarized decay provides a basis for an extensive discussion of available theories. In spite of good curve fitting capability, the empirical Williams–Watts expression should be discarded, because of too large variations of best-fit parameters upon changes in the fitting window. Valeur, Jarry, Geny, and Monnerie's model fits the data only in the long-time region and should be discarded for a precise short-time analysis.

The theoretical weakness of the VJGM model demonstrated here experimentally for the first time was overcome later by Jones and Stockmayer and by Bendler and Yaris. Indeed, our results clearly demonstrate the practical importance of these improvements: both models account satisfyingly for the orientational motions of polystyrene in solutions of various viscosities and using several fitting windows. But both models are also difficult to interpret because of arbitrary truncation procedures. On the other hand, the model recently proposed by Hall and Helfand, which relies on clear molecular assumptions, does not fit as well to the experiments. Using some empirical considerations and qualitative theoretical arguments, one can propose an expression for the orientational autocorrelation function closely related to Hall and Helfand's model, but more adapted to fluorescence decay experiments. In the case of polystyrene, this expression fits to the data as well as the BY and JS models, while keeping the attractive molecular basis of the HH model. Nevertheless, further theoretical work seems necessary to understand the exact physical meaning of this modification imposed by experiment.

Registry No. Polystyrene (homopolymer), 9003-53-6.

References and Notes

(1) G. Williams and D. C. Watts, *Trans. Faraday Soc.*, **66**, 80 (1971).
(2) B. Valeur, J. P. Jarry, F. Geny, and L. Monnerie, *J. Polym. Sci., Polym. Phys. Ed.*, **13**, 667, 675 (1975).
(3) A. A. Jones and W. H. Stockmayer, *J. Polym. Sci., Polym. Phys. Ed.*, **15**, 847 (1975).
(4) J. T. Bendler and R. Yaris, *Macromolecules*, **11**, 650 (1978).
(5) C. K. Hall and E. Helfand, *J. Chem. Phys.*, **77**, 3275 (1982).
(6) F. Perrin, *Ann. Phys.*, **12**, 169 (1929).
(7) P. E. Rouse, *J. Chem. Phys.*, **21**, 1272 (1953).
(8) P.-G. de Gennes, *Physics (Long Island City, N.Y.)*, **3**, 37 (1967).
(9) P. H. Verdier and W. H. Stockmayer, *J. Chem. Phys.*, **36**, 227 (1962).
(10) E. Dubois-Violette, F. Geny, L. Monnerie, and O. Parodi, *J. Chim. Phys. (Paris)*, **66**, 1865 (1969).
(11) B. I. Hunt and J. G. Powles, *Proc. Phys. Soc. London*, **88**, 513 (1966).
(12) J. E. Shore and R. Zwanzig, *J. Chem. Phys.*, **63**, 5445 (1975).
(13) R. Kimmich, *Polymer*, **16**, 851 (1975).
(14) J. C. Brochon, in "Protein Dynamics and Energy Transduction", Shin'ichi Ishiwata, Ed., Taniguchi Foundation, Japan, 1980.
(15) N. Tardiveau, These Docteur Ingenieur, Paris, 1980.
(16) B. Valeur and L. Monnerie, *J. Polym. Sci., Polym. Phys. Ed.*, **14**, 11, 29 (1976).
(17) See, for instance, P. Wahl, *Biophys. Chem.*, **10**, 91 (1979).
(18) NATO-ASI: "Time Resolved Fluorescence Spectroscopy in Biology and Biochemistry", St. Andrews, Scotland, 1980.
(19) IMSL Fortran Subroutines Library, IMSL, Houston, TX.
(20) R. Fletcher, "Fortran Subroutines for Minimization by Quasi-Newton Methods", Report AERE R7125, Harwell, England, 1972.
(21) P. R. Bevington, "Data Reduction and Error Analysis for the Physical Sciences", McGraw-Hill, New York, 1969.
(22) M. Bouchy, J. Y. Jezequel, J. C. Andre, and J. Bordet, Proceedings of the "Workshop on Deconvolution and Reconvolution of Analytical Signals", Nancy, May 22–23, 1982, M. Bouchy, Ed., ENSIC-INPL, Nancy, France.
(23) K. Kinosita, S. Kawato, and A. Ikegami, *Biophys. J.*, **20**, 289 (1977).
(24) A. Kawski, *Bull. Acad. Pol. Sci., Ser. Sci., Math., Astron. Phys.*, **6**, 533 (1958); L. A. Spektrov, *Dokl. Akad. Nauk SSSR*, **65**, 485 (1949).
(25) T. A. Weber and E. Helfand, to be published.

Concentration Dependence of the First Cumulant as a Function of Momentum Transfer

Boualem Hammouda

Department of Nuclear Engineering, The University of Michigan, Ann Arbor, Michigan 48109

A. Ziya Akcasu*,†

Center for Material Sciences, National Bureau of Standards, Washington, DC 20234.

Received March 17, 1983

ABSTRACT: Zimm's single-contact approximation is used to derive an expression for the concentration dependence of the first cumulant for dilute polymer solutions. The concentration dependence coefficient is found to decrease as a function of momentum transfer. This means that the concentration effect on the first cumulant is less important for smaller portions of polymer chains.

Introduction

A good deal of effort has been generated to study the concentration dependence of static as well as dynamic quantities characterizing polymer molecules in solution. Theoretical investigations tend to concentrate on the calculation of the concentration correction (in dilute solutions, for example) for directly measurable quantities, namely, the static structure factor or the dynamic structure factor and quantities that are related to them such as the first cumulant considered here.

In the case of the static structure factor $S(q)$, Zimm's[1] single-contact approximation is probably the first ap-

† Permanent address: Department of Nuclear Engineering, The University of Michigan.

0024-9297/83/2216-1852$01.50/0